Eutherian mammals use diverse strategies to initiate X-chromosome inactivation during development

Ikuhiro Okamoto, Catherine Patrat, Dominique Thepot Thépot, Nathalie Peynot, Patricia Fauque, Nathalie Daniel, Patricia Diabangouaya, Jean-Philippe Wolf, Jean Paul Renard, Véronique Duranthon, et al.

Eutherian mammals use diverse strategies to initiate X-chromosome inactivation during development

Ikuhiro Okamoto[1]*, Catherine Patrat[1,2]*, Dominique Thépot[3], Nathalie Peynot[3], Patricia Fauque[4,5], Nathalie Daniel[3], Patricia Diabangouaya[1], Jean-Philippe Wolf[6], Jean-Paul Renard[3], Véronique Duranthon[3] & Edith Heard[1]

X-chromosome inactivation (XCI) in female mammals allows dosage compensation for X-linked gene products between the sexes[1]. The developmental regulation of this process has been extensively investigated in mice, where the X chromosome of paternal origin (Xp) is silenced during early embryogenesis owing to imprinted expression of the regulatory RNA, *Xist* (X-inactive specific transcript). Paternal XCI is reversed in the inner cell mass of the blastocyst and random XCI subsequently occurs in epiblast cells. Here we show that other eutherian mammals have very different strategies for initiating XCI. In rabbits and humans, the *Xist* homologue is not subject to imprinting and XCI begins later than in mice. Furthermore, *Xist* is upregulated on both X chromosomes in a high proportion of rabbit and human embryo cells, even in the inner cell mass. In rabbits, this triggers XCI on both X chromosomes in some cells. In humans, chromosome-wide XCI has not initiated even by the blastocyst stage, despite the upregulation of *XIST*. The choice of which X chromosome will finally become inactive thus occurs downstream of *Xist* upregulation in both rabbits and humans, unlike in mice. Our study demonstrates the remarkable diversity in XCI regulation and highlights differences between mammals in their requirement for dosage compensation during early embryogenesis.

Most eutherian mammals display random XCI in their soma[1], whereas marsupials show imprinted, paternal XCI[2]. In mice, however, XCI is also imprinted initially, with silencing of Xp from the 4–8-cell stage[3–6]. Xp remains inactive in the trophectoderm[7] but is reactivated in the inner cell mass[5,6] (ICM) with subsequent random XCI in epiblast cells. Initiation of XCI is controlled by the non-coding *Xist* transcript[8,9], which coats the chromosome in *cis* and triggers gene silencing. During murine pre-implantation development, *Xist* is maternally repressed and paternally expressed, consistent with its role in regulating imprinted XCI[3,4,6,9,10]. By the epiblast stage, the imprint is lost or ignored, Xp has been reactivated and *Xist* can be upregulated randomly, from either Xp or the maternally derived X chromosome, Xm. This second, random wave of XCI involves downregulation of pluripotency factors, activation of *Xist* by means of X-linked competence factors and precise, random monoallelic regulation of *Xist*, possibly through antisense transcription, homologous pairing and other events (for a review, see ref. 11). Mice are the only eutherian for which XCI has been analysed in detail during early embryogenesis. The fact that marsupials also show XCI and yet have no gene homologous to *Xist* (refs 12, 13 and references therein) suggests that multiple strategies for initiating XCI must exist. To explore XCI during early embryogenesis in other eutherian mammals, we analysed human (primate) and rabbit (lagomorph) embryos, the latter being closely related to rodents[14].

First we examined rabbit embryos *in vivo*, from the 4-cell stage to the blastocyst stage, using *Xist* RNA fluorescence *in situ* hybridization (FISH; Fig. 1 and Supplementary Fig. 1). Sex chromosome constitution was determined after RNA FISH, by DNA FISH using X- and Y-chromosome probes. Punctate *Xist* RNA signals could be detected from both X chromosomes in females and from the single X chromosome in males, from the 8-cell stage (Fig. 1b, d), which corresponds to major embryonic genome activation (EGA) in rabbits[15,16]. This contrasts with mice, where maternal *Xist* is never expressed[4,6,11] between major EGA (the 2-cell stage[17]) and the blastocyst stage. *Xist* RNA accumulation was first detected in female, but not male, embryos at the morula stage (62 hours post-coitum (h.p.c.); about 60–70 cells). However, the percentage of female blastomeres showing *Xist* expression was low at this stage (Fig. 1c, d). By the early blastocyst stage (96 h.p.c.; Fig. 2a), over 90% of trophectoderm cells had at least one *Xist* RNA domain (Fig. 2a, c). Surprisingly, a substantial proportion of blastomeres (26%) showed *Xist* RNA domains on both X chromosomes (Fig. 2a, c). The detection of double *Xist* RNA domains in rabbit blastocysts contrasts with mouse, where such a situation is not usually seen *in vivo*[4–6] except in polyploid trophectoderm cells or in a low percentage (<4%) of *in vitro* differentiating female embryonic stem cells[18]. This unusual pattern is transient, however, as it is no longer observed in trophectoderm cells of 120 h.p.c. blastocysts (Fig. 2b), where a single *Xist* RNA domain is seen, as in XX somatic cells (Supplementary Fig. 2). In male rabbit embryos, *Xist* RNA domains were rarely detected (Fig. 2c). Instead, *Xist* was progressively silenced after the 8-cell stage (Fig. 2b, c). Thus, *Xist* upregulation is sensitive to XX status in rabbits, as in mice during random XCI, but *Xist* monoallelic regulation differs between the two animals.

During mouse development, X-linked gene silencing follows *Xist* RNA accumulation[3–6]. However, the timing of XCI in other mammals is less clear. We investigated expression of two X-linked genes using RNA FISH in rabbit embryos: *Hprt1* (also known as *Hprt*), which is X-inactivated in somatic cells, and *Jarid1c* (*Kdm5c*), which escapes XCI (Supplementary Fig. 2b). Expression of both genes was biallelic in female embryos from the 4–16-cell stage (Fig. 1). Thus, X-linked genes are active from both Xp and Xm at EGA, as in mice[4,6].

Hprt1 silencing on the *Xist*-RNA-coated chromosome was first detectable at the 96-h.p.c. blastocyst stage and was complete in trophectoderm cells by the 120-h.p.c. stage (Fig. 2d), whereas *Jarid1c* still showed biallelic expression indicating escape from XCI, as in somatic cells. Importantly, the onset of *Hprt1* silencing coincided with the time window (96 h.p.c.) when both X chromosomes were sometimes found to be *Xist* RNA coated (Fig. 2a). Indeed, by comparing the proportion of cells showing no *Hprt1* primary transcript signal and two *Xist* RNA domains with those showing a single *Xist* RNA domain (46%, $n = 192$ versus 12%, $n = 250$), we conclude that *Hprt1* silencing has initiated on both X chromosomes in cells with two *Xist* RNA domains at the 96-h.p.c. stage (Fig. 2e). This situation was found to be rapidly reversed

[1]Mammalian Developmental Epigenetics Group, Institut Curie, CNRS UMR 3215, INSERM U934, Paris 75248, France. [2]Université Paris Diderot – Assistance Publique Hôpitaux de Paris – Service de Biologie de la Reproduction, Hôpital Bichat-Claude Bernard, 75018 Paris, France. [3]INRA UMR 1198 Biologie du Développement et de la Reproduction, F-78352 Jouy en Josas Cedex, France. [4]Laboratoire de Biologie de la reproduction CECOS, CHU de Dijon, Université de Bourgogne, 21079 Dijon, France. [5]Epigenetic Decisions and Reproduction in mammals, Institut Curie, CNRS UMR 3215, INSERM U934, 75248 Paris, France. [6]Unité Inserm 1016, Université Paris Descartes – Assistance Publique Hôpitaux de Paris – Service de Biologie de la Reproduction, Hôpital Cochin, 75014 Paris, France.
*These authors contributed equally to this work.

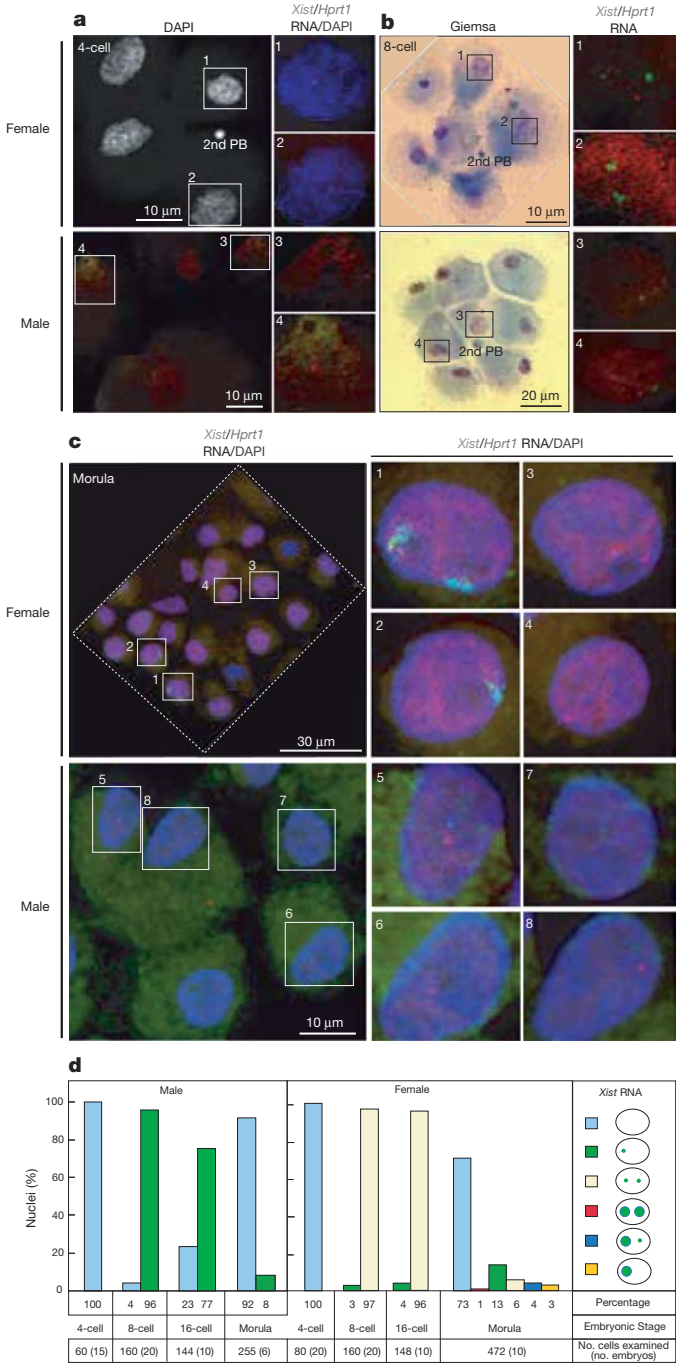

Figure 1 | *Xist* and *Hprt1* expression in early pre-implantation rabbit embryos. Examples of embryos after RNA FISH for *Xist* RNA (green) and X-linked *Hprt1* primary transcripts (red). An intact male or female embryo and several representative nuclei are shown. **a**, Representative 4-cell embryos: XX (nuclei 1 and 2) and XY (nuclei 3 and 4) blastomeres. DAPI, 4′,6-diamidino-2-phenylindole; PB, polar body. **b**, Representative 8-cell embryos: XX (nuclei 1 and 2) and XY (nuclei 3 and 4) blastomeres. **c**, Representative XX (nuclei 1–4) and XY (nuclei 5–6) morula-stage embryos. **d**, Percentage of cells showing different *Xist* expression patterns in the 4-cell to morula stages. The low percentage of *Xist* RNA detection in morulae is not a technical issue, as *Hprt1* primary transcript signals could be efficiently detected at this stage in most male and female blastomeres.

24 h later (at the 120-h.p.c. stage), as only one X chromosome showed *Xist* RNA coating and *Hprt1* silencing; the other expressed *Hprt1* in almost all blastomeres (Fig. 2b).

We also analysed histone H3 lysine 27 trimethylation (H3K27me3) enrichment, which marks the onset of XCI in mice[19,20] and is present on the inactive X chromosome in rabbit somatic cells (Supplementary Fig. 2c). In 96-h.p.c. blastocysts, where two *Xist*-RNA-coated X chromosomes could be detected (25%, $n = 325$), both of them showed H3K27me3 enrichment (Supplementary Fig. 3). At the 120-h.p.c. stage, where only one *Xist* RNA domain is detectable, two spots of H3K27me3 staining per nucleus could still sometimes be observed (8%, $n = 285$), one overlapping with *Xist* RNA and the other presumably corresponding to the second X chromosome (Supplementary Fig. 3).

Taken together, these results suggest that XCI initiates on both X chromosomes in a significant proportion of blastomeres in early rabbit blastocysts, but the situation is somehow resolved. As no differences in cell death rates could be detected between female and male 120-h.p.c. embryos (Supplementary Fig. 4), we conclude that cells initiating XCI on both X chromosomes do not necessarily die. They either reverse XCI on one X chromosome or proliferate more slowly and become out-competed by cells with one inactive X chromosome, which is a distinct possibility given the massive cell proliferation occurring between 96 h.p.c. (~100 cells) and 120 h.p.c. (>1,000 cells; Fig. 2f).

We also analysed the ICMs of rabbit blastocysts for XCI status. In mice, inactive Xp is progressively reactivated in pre-epiblast ICM cells[5,6] positive for Oct4 (Pou5f1) and Nanog[6]. Rabbit ICM cells were isolated from blastocysts by immunosurgery or manual dissection. In early blastocysts (96 h.p.c.), most putative ICM cells were negative for *Xist* RNA accumulation (Supplementary Fig. 5a, c), in contrast to trophectoderm cells, where *Xist* RNA coating of one or both X chromosomes was present in most cells (Fig. 2a). One day later (120 h.p.c.), however, the majority of putative (strongly Oct4-positive) epiblast cells displayed *Xist* RNA coating on one or both X chromosomes, as well as the onset of *Hprt1* gene silencing and H3K27me3 enrichment (Supplementary Fig. 5).

Thus, in rabbits, two waves of XCI with similar characteristics seem to occur, one in the trophectoderm and the second in the ICM. During both waves, the two X chromosomes seem to be affected initially in some cells, implying that there is no imprinting, unlike in the mouse. However, we could not analyse parent-specific X-linked gene expression owing to lack of polymorphisms in our rabbit colonies. Instead, we investigated rabbit parthenogenotes (two maternal genomes) for their XCI patterns. We found *Xist* and *Hprt1* expression patterns similar to those of wild-type female embryos (Supplementary Fig. 6), indicating that imprinting may not have a major role in rabbit XCI, but we cannot formally exclude that there is some parent-of-origin bias. In summary, we show that although rabbits and mice are phylogenetically close, they have taken very different evolutionary trajectories with respect to *Xist* regulation and the onset of XCI.

In human embryos, *XIST* expression is detected from the 4–8-cell stage and XCI has been proposed to follow kinetics similar to those in mouse[21], although it does not seem to be imprinted in extra-embryonic tissues[22,23]. To investigate this further, we examined *in vitro* conceived pre-implantation human embryos (Fig. 3; Methods and Supplementary Information). Human blastocysts showed either a single or double *XIST* RNA accumulation (67% cells, $n = 13$ embryos and 85% cells, $n = 15$ embryos, respectively; Fig. 3a), corresponding to male and female embryos, confirmed by X/Y DNA FISH (Fig. 3a). Similar *XIST* patterns were detected in morulae and blastocysts (days 5 and 6), whether derived by IVF (*in vitro* fertilization) or ICSI (intracytoplasmic sperm injection), and whatever their history (discarded or frozen-thawed embryos).

To assess XCI status, X-linked genes (*ATRX*, *FGD1* and *HUWE1*) were analysed by RNA FISH. In human somatic cells, these genes are silent on the inactive X chromosome (Supplementary Fig. 7). In female blastocysts, the majority of blastomeres showed two primary transcript foci for X-linked genes (*ATRX* and *FGD1*, Fig. 3a, e; *HUWE1*, data not shown), indicating that both X chromosomes are active. Furthermore, although small foci of H3K27me3 enrichment could be detected throughout the nucleus, no specific enrichment on the *XIST*-coated chromosomes was found (Fig. 3b).

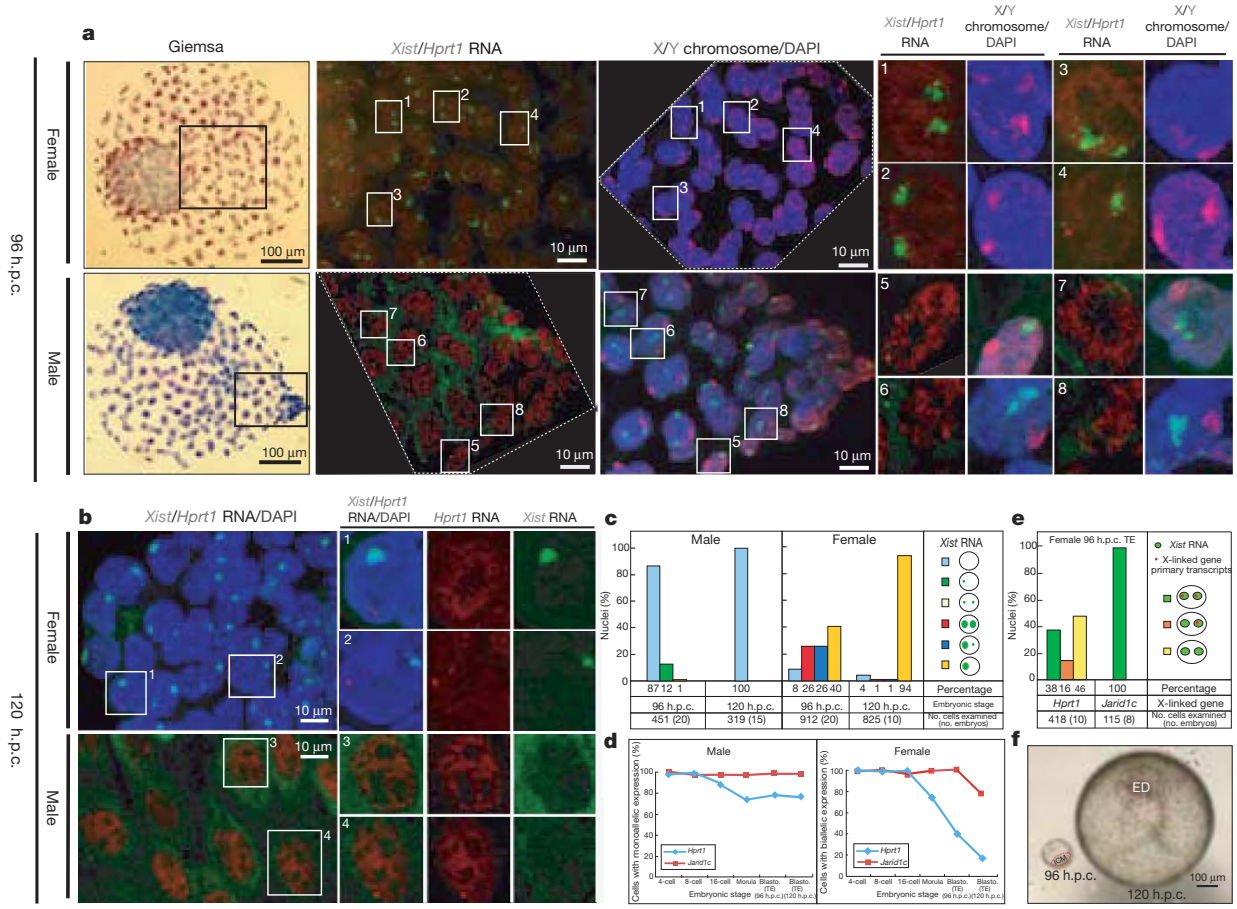

Figure 2 | *Xist* and *Hprt1* expression in early- (96-h.p.c.) and late-stage (120-h.p.c.) rabbit blastocysts. Examples of embryos (Giemsa-stained) analysed by RNA FISH to detect *Xist* (green) and *Hprt1* (red), followed by DNA FISH using X-chromosome (red) and Y-chromosome (green) probes. Intact male and female embryos, together with representative nuclei, are shown. **a**, Individual XX and XY early (96-h.p.c.) blastocysts: representative XX (nuclei 1–4) and XY (nuclei 5–8) cells. **b**, Late XX and XY blastocysts: representative XX (nuclei 1 and 2) and XY (nuclei 3 and 4) blastomeres. **c**, Percentage of cells showing different *Xist* expression patterns in rabbit embryos at early and late blastocyst stages. **d**, Average percentage of blastomeres showing primary transcripts for *Hprt1* or *Jarid1c* in female and male embryos from the 4-cell stage to the blastocyst stage ($n \geq 10$, each stage). TE, trophectoderm. **e**, Summary of X-linked gene expression patterns in blastomeres with double *Xist* RNA domains in early female blastocysts. **f**, Phase contrast images of living early (day-4, 96-h.p.c.) and late (day-5, 120-h.p.c.) rabbit blastocysts. ED, embryonic disc.

We also analysed a few even later human blastocysts (cultured to day 7). Male, day-7 blastocysts showed either no (66%, $n = 271$ cells, $n = 2$ embryos) or just a small punctate *XIST* RNA signal (Supplementary Fig. 8), suggesting that *XIST* expression was downregulated by this stage. A heterochromatic Y body[24] was also visible in these embryos. In the one female embryo obtained at day 7, the majority of cells still showed biallelic *FGD1* expression (83%, $n = 30$ cells) and biallelic *XIST* RNA signals, with no sign of a heterochromatic Barr body (Supplementary Fig. 8).

A previous study reported that XCI can be detected in early human embryos[21]. The discrepancy with our study may be due to differences in immunofluorescence/FISH techniques resulting in less efficient detection of biallelic RNA signals, for example, and/or to different culture conditions (see Supplementary Information for discussion). There is also some debate concerning XCI status in human embryonic stem cells. A recent study[25] reported that human embryonic stem cells cultured in 5% oxygen retain pre-XCI cells, whereas in atmospheric oxygen *XIST* upregulation and an inactive X chromosome are often found. However, this may be specific to the tissue culture conditions of human embryonic stem cells. We therefore analysed the ICM in both male and female human embryos. Putative ICM cells (strongly OCT4 positive) showed similar *XIST* RNA patterns to surrounding trophectoderm cells and no sign of an inactive X chromosome ($n = 4$ embryos; Fig. 3b). We conclude that in human pre-implantation embryos, under our conditions, *XIST* RNA upregulation occurs on all X chromosomes regardless of parental origin or sex but does not seem to result in chromosome-wide XCI even in late blastocysts. Although we cannot rule out that *in vitro* culture and atmospheric oxygen might have an impact on XCI, in our conditions the X seems to be in a pre-XCI state in human ICM cells, in agreement with ref. 25.

In conclusion, our findings reveal substantial diversity in the timing and regulation of XCI initiation between mammals (Supplementary Fig. 9a). First, *Xist* expression is not imprinted in early rabbit and human embryos, unlike in mice. The maternal *Xist* imprint found in mice may therefore be a recent event, which we have proposed[26] evolved to avoid premature maternal XCI given the early onset of EGA and *Xist* expression. Indeed, in mouse XpXp androgenotes, which lack an imprinted maternal Xm, *Xist* is upregulated biallelically initially, as in rabbits and humans[27]. However, rabbits and humans have later EGA and may not require *Xist* imprinting for early XCI control. Second, the choice of which X chromosome to inactivate seems to occur downstream of *Xist* upregulation in rabbits and humans, unlike in mice, where *Xist* is tightly monoallelically regulated during random XCI (Supplementary Fig. 9b). One difference could be that antisense transcription (*Tsix*), which is critical for random, monoallelic *Xist* expression in mice[28], is poorly conserved and may even be lacking in other mammals[29].

Another difference between human and rabbit or mouse embryos is that *XIST* upregulation occurs in males and females, suggesting that

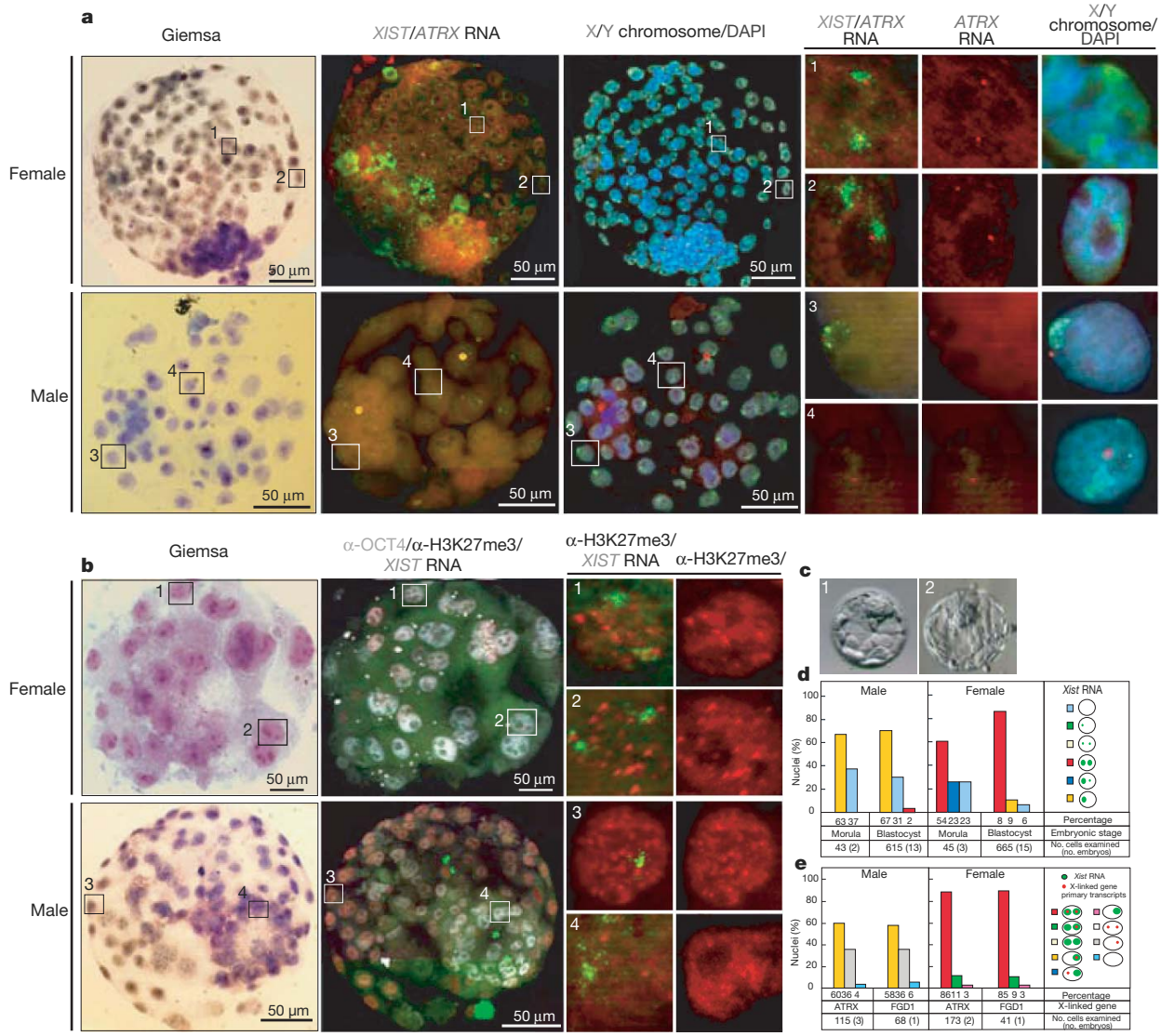

Figure 3 | *XIST* RNA, X-linked gene expression and H3K27me3 profiles in human blastocysts. **a**, Examples of individual female and male human embryos (Giemsa) analysed by RNA FISH for *XIST* RNA (green) and primary transcription from the X-linked *ATRX* gene (red), followed by DNA FISH for the X chromosome (red) and Y centromere (green). Representative XX (nuclei 1 and 2) and XY blastomeres (nuclei 3 and 4) are shown. Zones of intense green signal outside nuclei are background. **b**, Examples of individual female and male human embryos (Giemsa) analysed by immunolabelling with antibodies against H3K27me3 (red) and OCT4 (white), combined with *XIST* RNA FISH (green). For each sex, an intact embryo (Giemsa, immunofluorescence/RNA FISH) together with several enlarged nuclei are shown: representative XX (nuclei 1 and 2) and XY blastomeres (nuclei 3 and 4). **c**, Phase contrast images of an expanding blastocyst (left) and a fully expanded blastocyst (right). **d**, Percentage of cells showing different *XIST* expression patterns in morula- to blastocyst-stage embryos. **e**, Percentage of female and male blastocyst cells showing different X-linked gene expression patterns in blastomeres with *XIST* RNA domains.

XIST activators are not XX-specific, at least initially (Supplementary Fig. 9a). However, *XIST* upregulation is dissociated from the immediate onset of chromosome-wide XCI, possibly as a result of incomplete *XIST* RNA *cis*-coating. Indeed, *XIST* RNA signals were quite diffuse in human embryos (Fig. 3) in comparison with somatic cells (Supplementary Fig. 7). Importantly, the lack of chromosome-wide XCI in the trophectoderm of human blastocysts implies that dosage compensation may not be critical at this stage.

Finally, we also reveal differences between mammals in XCI status in the ICM. In humans the two X chromosomes seem to be active in the ICM (even though *XIST* is expressed), whereas in rabbits the two X chromosomes are initially active and then become inactive. This is the reverse situation to mice, where Xp is initially inactive and then becomes reactivated in the ICM[6]. These differences may explain the diverse XCI patterns reported in embryonic stem cells of non-murine mammals and point to differences in *Xist* control via pluripotency factors[30]. The diversity of XCI initiation strategies we have uncovered here probably reflects the fact that developmental processes are constantly changing during evolution and that the regulation of processes such as XCI have to display substantial plasticity to accommodate these changes.

METHODS SUMMARY

Human and rabbit embryos were manipulated under strict ethical guidelines and analysed using published protocols for immunostaining, RNA and DNA FISH[6,26]. Human embryos obtained following IVF or ICSI were cultured in 5% CO_2 and atmospheric O_2, fixed and used for immunofluorescence or RNA FISH, as previously described[6]. Rabbit embryos were obtained from superovulated New Zealand White rabbit females mated with males. *In vivo* rabbit embryos were recovered from oviducts or uterus flushed with PBS at appropriate times post-coitum. The mucin coat and zona pellucida were removed before fixation for immunofluorescence/FISH[6]. Rabbit ICMs (96 h.p.c.) were isolated by immunosurgery; embryonic discs (120 h.p.c.) were dissected out with tungsten needles.

Full Methods and any associated references are available in the online version of the paper at www.nature.com/nature.

1. Lyon, M. F. Gene action in the X-chromosome of the mouse (*Mus musculus* L.). *Nature* **190,** 372–373 (1961).
2. Sharman, G. B. Late DNA replication in the paternally derived X-chromosome of female kangaroos. *Nature* **230,** 231–232 (1971).
3. Huynh, K. D. & Lee, J. T. Inheritance of a pre-inactivated paternal chromosome in early mouse embryos. *Nature* **426,** 857–862 (2003).
4. Patrat, C. *et al.* Dynamic changes in paternal X-chromosome activity during imprinted X-chromosome inactivation in mice. *Proc. Natl Acad. Sci. USA* **106,** 5198–5203 (2009).
5. Mak, W. *et al.* Reactivation of the paternal X chromosome in early mouse embryos. *Science* **303,** 666–669 (2004).
6. Okamoto, I., Otte, A. P., Allis, C. D., Reinberg, D. & Heard, E. Epigenetic dynamics of imprinted X inactivation during early mouse development. *Science* **303,** 644–649 (2004).
7. Takagi, N. & Sasaki, M. Preferential inactivation of the paternally derived X-chromosome in the extraembryonic membranes of the mouse. *Nature* **256,** 640–642 (1975).
8. Penny, G. D., Kay, G. F., Sheardown, S. A., Rastan, S. & Brockdorff, N. Requirement for *Xist* in X chromosome inactivation. *Nature* **379,** 131–137 (1996).
9. Marahrens, Y., Panning, B., Dausman, J., Strauss, W. & Jaenisch, R. *Xist*-deficient mice are defective in dosage compensation but not spermatogenesis. *Genes Dev.* **11,** 156–166 (1997).
10. Kay, G. F., Barton, S. C., Surani, M. A. & Rastan, S. Imprinting and X chromosome counting mechanisms determine Xist expression in early mouse development. *Cell* **77,** 639–650 (1994).
11. Navarro, P. & Avner, P. An embryonic story: analysis of the gene regulative network controlling Xist expression in mouse embryonic stem cells. *Bioessays* **32,** 581–588 (2010).
12. Duret, L., Chureau, C., Samain, S., Weissenbach, J. & Avner, P. The Xist RNA gene evolved in eutherians by pseudogenization of a protein-coding gene. *Science* **312,** 1653–1655 (2006).
13. Okamoto, I. & Heard, E. Lessons from comparative analysis of X-chromosome inactivation in mammals. *Chromosome Res.* **17,** 659–669 (2009).
14. Hajjoubi, S. *et al.* Ruminants genome no longer contains Whey Acidic Protein gene but only a pseudogene. *Gene* **370,** 104–112 (2006).
15. Manes, C. The participation of the embryonic genome during early cleavage in the rabbit. *Dev. Biol.* **32,** 453–459 (1973).
16. Christians, E., Rao, V. H. & Renard, J. P. Sequential acquisition of transcriptional control during early embryonic development in the rabbit. *Dev. Biol.* **164,** 160–172 (1994).
17. Flach, G. *et al.* The transition from maternal to embryonic control in the 2-cell mouse embryo. *EMBO J.* **1,** 681–686 (1982).
18. Monkhorst, K., Jonkers, I., Rentmeester, E., Grosveld, F. & Gribnau, J. X inactivation counting and choice is a stochastic process: evidence for involvement of an X-linked activator. *Cell* **132,** 410–421 (2008).
19. Plath, K. *et al.* Role of histone H3 lysine 27 methylation in X inactivation. *Science* **300,** 131–135 (2003).
20. Silva, J. *et al.* Establishment of histone h3 methylation on the inactive X chromosome requires transient recruitment of Eed-Enx1 polycomb group complexes. *Dev. Cell* **4,** 481–495 (2003).
21. van den Berg, I. M. *et al.* X chromosome inactivation is initiated in human preimplantation embryos. *Am. J. Hum. Genet.* **84,** 771–779 (2009).
22. Migeon, B. X-chromosome inactivation: theme and variations. *Cytogenet. Genome Res.* **99,** 8–16 (2002).
23. Moreira de Mello, J. C. *et al.* Random X inactivation and extensive mosaicism in human placenta revealed by analysis of allele-specific gene expression along the X chromosome. *PLoS ONE* **5,** e10947 (2010).
24. Barlow, P. & Vosal, C. G. The Y chromosome in human spermatozoa. *Nature* **226,** 961–962 (1970).
25. Lenger, C. J. *et al.* Derivation of pre-X inactivation human embryonic stem cells under physiological oxygen concentrations. *Cell* **141,** 1–12 (2010).
26. Okamoto, I. *et al.* Evidence for de novo imprinted X-chromosome inactivation independent of meiotic inactivation in mice. *Nature* **438,** 369–373 (2005).
27. Okamoto, I., Tan, S. & Takagi, N. X-chromosome inactivation in XX androgenetic mouse embryos surviving implantation. *Development* **127,** 4137–4145 (2000).
28. Lee, J. T. Regulation of X-chromosome counting by *Tsix* and *Xite* sequences. *Science* **309,** 768–771 (2005).
29. Chang, S. C. & Brown, C. J. Identification of regulatory elements flanking human XIST reveals species differences. *BMC Mol. Biol.* **11,** 20 (2010).
30. Navarro, P. *et al.* Molecular coupling of *Xist* regulation and pluripotency. *Science* **231,** 1693–1695 (2008).

Acknowledgements We thank members of the Heard lab for advice and discussions, V. Colot for comments on the manuscript, and P. Jouannet and Hôpital Cochin's IVF unit for support and advice on human embryo experiments. We are indebted to the Unité Commune d'Expérimentation Animale in charge of the rabbit colonies, C. Archilla for technical help in sexing rabbit embryos, C. Rogel-Gaillard for providing rabbit bacterial artificial chromosomes before publication, and the UMR3215 PICT-IBiSA imaging facility. Funding is from the FRM (Equipe FRM), the ANR and the ERC (E.H.); the Agence de Biomedecine (C.P. and P.F.); and the INRA PHASE department (ACI 2007) (V.D. and J.-P.R.).

Author Contributions E.H., I.O., J.-P.R., V.D. and C.P. designed the experiments. I.O. performed immunofluorescence and FISH experiments on both rabbit and human embryos; C.P. and P.D. performed some of the FISH experiments on human embryos. C.P. obtained the license to work with human embryos and interviewed couples to obtain consent for use of discarded embryos. C.P. and P.F. performed the human IVF and ICSI experiments and manipulated the human embryos. J.-P.W. directed the laboratory in which the human embryos were made available. D.T. screened rabbit bacterial artificial chromosome libraries, provided rabbit probes and conducted comparative sequence analysis. N.P., N.D. and V.D. obtained and manipulated rabbit embryos. J.-P.R. directed the laboratory in which the rabbit embryos were obtained and manipulated. I.O., C.P., D.T., V.D. and E.H. analysed the data. I.O. and E.H. wrote the manuscript together with input from V.D. and C.P.

METHODS

Recovery of pre-implantation rabbit embryos. Experiments were performed in accordance with the International Guiding Principles for Biomedical Research involving animals, as promulgated by the Society for the Study of Reproduction and with the European Convention on Animal Experimentation. Researchers involved in direct work with the animals possessed an animal experimentation licence delivered by the French veterinary services. New Zealand White rabbit females (INRA line 1077) were superovulated and mated with normal males. Superovulation was performed by five subcutaneous injections of pFSH (Stimufol, Merial Lyon) for three days before mating: two 5-µg injections on day 1 at 12-h intervals, two 10-µg injections on day 2 at 12-h intervals and one 5-µg injection on day 3, followed 12 h later by an intravenous injection of 30 IU human chorionic gonadotrophin (Chorulon, Intervet) at mating time. *In vivo*, four-cell, eight-cell, sixteen-cell and morula-stage embryos were recovered from oviducts and uterus flushed with PBS at 30, 38, 46, 62–72 h.p.c., respectively. Uterus flushing was at 96 and 120 h.p.c. for the recovery of early and late blastocysts, respectively. Mucin coat was removed by incubation of the embryos in a pre-warmed pronase solution (0.5% Protease, Sigma) at 37 °C for 1 to 6 min depending on its thickness and on the stage of the embryo. Embryos were then immediately rinsed twice in M199 HEPES with 10% FCS. In the second wash, the zona pellucida was removed by mechanical pipetting. For immunofluorescence and RNA FISH, embryonic discs were dissected out from the late (120-h.p.c.) blastocysts with tungsten needles.

ICM isolation from early (96-h.p.c.) rabbit blastocyst. Mucin coat and zona pellucida were removed by pronase treatment of blastocysts. ICMs were then isolated by immunosurgery. Briefly, embryos were incubated in anti-rabbit goat serum (Sigma R-5131) for one hour at 37 °C. They were then rinsed twice in PBS and incubated in guinea pig complement (Sigma S-1639) for one to two minutes. Blastocysts were then rinsed in PBS and vacuolated trophectoderm cells were mechanically removed by pipetting with a small adjusted pipette (70–90-µm diameter).

Parthenogenetic activation of rabbit embryos. *In vitro* activation was performed on morphologically normal, fresh MII oocytes (14 h.p.c.), as previously described[31,32] for nuclear transfer experiments. Briefly, oocytes were washed three times in the TCM199, HEPES plus 10% FCS and placed in a mannitol solution containing 0.3 M mannitol, 100 µM $MgCl_2$ and 100 µM $CaCl_2$ in sterile, filtered water. After 30 s in the mannitol solution, oocytes were 'electroactivated' with a succession of three d.c. pulses of 3.2 kV cm^{-1} for 20 µs each, using a BTX stimulator (Biotechnologies & Experimental Research). Then oocytes were incubated for 1 h in TCM199 plus 10% FCS at 38.5 °C and 5% CO_2 in a humidified atmosphere. Then they received, in the mannitol solution, a second set of three d.c. pulses and were incubated for 1 h in TCM199 plus 10% FCS supplemented with 2 mM 6-DMAP (kinase inhibitor) and 5 µg $µl^{-1}$ cycloheximid (protein synthesis inhibitor) to finalize activation. Lastly, they were washed three times in the TCM199 plus 10% FCS to remove all traces of chemical agents, and were rinsed for 30 min in TCM199 plus 10% FCS at 38.5 °C and 5% CO_2. They were then incubated in microdrops of B2 plus 2.5% FCS under mineral oil at 38.5 °C and 5% CO_2.

Recovery of human pre-implantation embryos. All attempts using assisted reproductive techniques were performed at Cochin-Saint Vincent Hospital (Paris, France). Ovarian stimulation, oocyte retrieval, sperm processing and IVF and/or ICSI were performed as previously described[33]. The choice of ICSI or conventional IVF as fertilization method was dependent on semen-sample characteristics and couple's history. Briefly, oocytes retrieval was performed under vaginal ultrasound guidance, 36 h after administration of human chorionic gonadotrophin. Motile spermatozoa were selected through a two-step 90–45% density gradient (Puresperm, JCD) or after sperm washing with FertiCult medium (JCD). On the day of oocyte retrieval, sperm-inseminated or -microinjected oocytes were cultured in 30 µl culture medium (IVF or ISM1, Origio) under oil, at 37 °C, 5% CO_2 and humidified atmosphere. Fertilization was assessed 18 h after insemination or injection and normal fertilization was defined as the presence of two distinct pronuclei and a second polar body. Embryo quality was evaluated on day 2 or day 3 according to the number of blastomeres, the degree of fragmentation and the presence or not of multinuclear blastomeres. Embryos were either transferred or cryopreserved on day 2 or day 3, depending on the embryo quality evaluation. Embryos that were neither transferred nor cryopreserved, given poor embryo morphology, were discarded.

Collection of human embryos. Research on human embryos was authorized by the French Biomedicine Agency (RE07-011R). In the present study, only diploid embryos that were either discarded or cryopreserved were used. In both cases, written consent was obtained from the couples allowing these discarded or cryopreserved embryos to be used for the research. Embryos (after thawing (Embryo Thawing Pack, Origio), for day-2–3 cryopreserved embryos) were placed in 30 µl of fresh, equilibrated sequential culture medium (ISM1 culture medium from day 2 to day 3 and ISM2 from day 3, Medicult) at 37 °C, 5% CO_2, under oil and humidified atmosphere, for further culture. Blastocysts were obtained at day 5 or day 6 post-insemination or -injection and classified according to Gardner's classification[34], taking into account the global morphology and ICM and trophectoderm aspect from mid blastocyst.

Rabbit probes. All rabbit bacterial artificial chromosomes (BACs) were isolated from a rabbit library maintained at the UR1313, Unité de Génétique Animale et Biologie Intégrative, Institut National de la Recherché Agronomique (INRA). *Hprt1* and *Jarid1c* BACs had been previously published[35,36]. *Xist*-containing BACs (573D5, 614B8 and 717B2) were isolated by a PCR-based screening protocol (C. Rogel-Gaillard, unpublished results). BACs were verified for their location and single-copy nature by DNA FISH on metaphase spreads. For *Xist* RNA FISH, shorter probes were derived from the BACs. First, the human *XIST* gene sequence was compared with discontinuous megaBLAST to rabbit whole-genome shotgun sequences from the Trace Archives of the NCBI site to identify homologous rabbit *Xist* sequences. Second, these genomic sequences were extracted and then assembled in six large sequences using the CAP3 assembly program[37]. These six large sequences encompass the promoter and beginning of exon 1 (4,090 base pairs (bp)), the middle of exon 1 (6,255 bp), the end of exon 1 and part of intron 1 (3,250 bp), from the end of intron 4 to more than 3 kb into exon 6 (5,792 bp), the middle of exon 6 (1,300 bp) and the end of exon 6 (2,067 bp), respectively. Finally, primers were designed to amplify large parts of the rabbit *Xist* gene from the BACs. For RNA FISH, a mixture of these three probes obtained from long-range PCR products (Roche) were amplified using the 8F/17R, 16F/3R and 6F/6R primers pairs, respectively (8F, 5′-TATAGGAATGCTGACCACTGA-3′; 17R, 5′-GTTTTTTCAGTCAAGGGAGAC-3′; 16F, 5′-TCATGCTCCTGAATCTTCTTG-3′; 3R, 5′-GCCGCACAAGGAAGAAAAAAG-3′; 6F, 5′-TGTGTATTTCTCTTTGTCTTT-3′; 6R, 5′-GTTCTCAAAGCAGTACATTTTTATTTTACAGTACACAAC 3′). The three PCR products encompass sequences from the middle of exon 1 to the end of intron 1 (~8 kb), the beginning of intron 1 to the beginning of exon 6 (~10 kb), and all of exon 6 (~7.3 kb) (Supplementary Fig. 1).

Human probes. BAC probes (Supplementary Table 2) were used following verification of their location and single-copy nature by DNA FISH on female human metaphases. Two DNA probes detecting *XIST* RNA were used: (i) a 10-kb fragment corresponding to *XIST* exon 1 (gift from C. Brown, Department of Medical Genetics, University of British Columbia) and (ii) a VI.34 Flp-In T-Rex *XIST* CDNA DH10B construct[38] (gift from C. Brown).

Immunofluorescence, RNA FISH and DNA FISH. Immunofluorescence and RNA FISH were carried out as described previously[6,26]. DNA FISH was performed following RNA FISH. The coverslips carrying the embryos were then recovered in ×2 SSC and incubated in RNase A (100 µg ml^{-1}) in ×2 SSC at 37 °C for 1 h, before a brief rinse in ×2 SSC, dehydration through an ethanol series and air drying. The coverslips were treated with 0.03% pepsin in 0.01 N HCl for 10–30 min at 37 °C to enhance the penetration of probes. After washing in PBS, they were dehydrated through an ethanol series. The DNA was then denatured in 70% formamide, ×2 SSC (pH 7.4) for 10 min at 80 °C and dehydrated again through an ice-cold ethanol series. Hybridization and revelation of the chromosome paint probes were performed according to manufacturer's instructions (Cambio). Cover slips were counterstained with DAPI (1 µg ml^{-1}), mounted and viewed under the fluorescence microscope.

TUNEL assay and sexing of rabbit embryos. *In vivo* developed blastocysts were recovered at 120 h.p.c. They were dissected into two halves. One half of each embryo was used for sexing by nested PCR against the *Sry* gene. Briefly, frozen hemi-embryos were lysed in 10 µl of TE buffer containing 0.01 mg ml^{-1} proteinase K and incubated in this buffer for 2 h at 56 °C. Proteinase K was then inactivated by heating at 94 °C for 10 min. PCR was then directly performed in a 50-µl final volume using Takara Taq DNA polymerase (Lonza) for 30 cycles using external primers (*Sry* F2 5′-gttcggagcactgtacagcg-3′ and *Sry* R2 5′-gcgttcatgggtcgcttgac-3′). A quantity (3 µl) of the first PCR reaction was then re-amplified in a 50-µl PCR reaction for 35 cycles using the internal primers (*Sry* F1 5′-tgcttacacaccagccaaaca-3′ and *Sry* R1 5′-ttcctggccgctcactttac-3′) (PCR cycles: 94 °C for 3 min, then 94 °C for 30 s, 58 °C for 30 s and 72 °C for 1 min). PCR products (20 µl) were analysed by electrophoresis on a 2% agarose gel. The other half of each embryo was underwent TUNEL assay using the DeadEnd Fluorometric TUNEL System (Promega). Briefly, hemi-embryos were fixed in paraformaldehyde (4%) overnight at 4 °C. After rinsing in PBS containing 0.2% BSA, they were incubated in 10 µg ml^{-1} Proteinase K for 2 min. After rinsing, they were fixed again in 4% paraformaldehyde and 0.2% glutaraldehyde for 15 min at room temperature (22 °C). They were then rinsed twice in PBS containing 0.2% BSA. Positive control embryos were treated by RQ1 RNase-free DNase for 10 min as recommended by the manufacturer. TUNEL reaction was then performed on all the embryos as recommended by the manufacturer. The embryos were then incubated for 10 min at room temperature in

10 μg ml^{-1} Hoechst (Sigma). They were rinsed in 0.2% BSA in PBS and mounted in Citifluor (Biovalley) before imaging.

Fluorescence microscopy. A 200M Axiovert (Zeiss) fluorescence microscope equipped with an ApoTome system was used for image acquisition and the generation of optical sections in three dimensions. Sequential *z*-axis images were collected in 0.3-μm steps. At the blastocyst stage, when possible, we distinguished cells corresponding to the trophectoderm or the ICM according to their morphology. Results were expressed as mean ± s.e.m.

31. Chesné, P. *et al.* Cloned rabbits produced by nuclear transfer from adult somatic cells. *Nature Biotechnol.* **20,** 366–369 (2002).
32. Challah-Jacques, M., Chesne, P. & Renard, J. P. Production of cloned rabbits by somatic nuclear transfer. *Cloning Stem Cells* **5,** 295–299 (2003).
33. Fauque, P. *et al.* Cumulative results including obstetrical and neonatal outcome of fresh and frozen-thawed cycles in elective single versus double fresh embryo transfers. *Fertil. Steril.* **94,** 927–935 (2010).
34. Gardner, D. K. & Schoolcraft, W. B. in *Towards Reproductive Certainty: Infertility and Genetics Beyond 1999* (eds Jansen, R. & Mortimer, D.) 378–388 (Parthenon, 1999).
35. Hayes, H. *et al.* Establishment of R-banded rabbit karyotype nomenclature by FISH localization of 23 chromosome-specific genes on both G- and R-banded chromosomes. *Cytogenet. Genome Res.* **98,** 199–205 (2002).
36. Chantry-Darmon, C. *et al.* 133 new gene localization on the rabbit cytogenetic map. *Cytogenet. Genome Res.* **103,** 192–201 (2003).
37. Huang, X. & Madan, A. CAP3: A DNA sequence assembly program. *Genome Res.* **9,** 868–877 (1999).
38. Chow, J. C. *et al.* Inducible XIST-dependent X-chromosome inactivation in human somatic cells is reversible. *Proc. Natl Acad. Sci. USA* **104,** 10104–10109 (2007).